RE-ENTRY STRATEGY ANALYSIS OF REUSABLE LAUNCH VEHICLES

Radu BLIDERAN[1], Andrei NEAMTU[2]

The paper presents the initial result of a project that aims to analyze the optimal re-entry trajectory of a reusable, streamlined spacecraft, equipped with aerodynamic control surfaces, with the aim of achieving interception/coupling by an specially designed UAV (Unmanned Aerial Vehicle). Three re-entry strategies are analyzed: Atmospheric re-entry using only controlled AOA (Angle of Attack), atmospheric re-entry using controlled AOA and Bank angle and suborbital flight from 60 km altitude to the interception conditions imposed (altitude of 10 km and 0.85 Mach). The results will serve as a basis for future development of the guidance and control algorithm necessary to achieve mid-air recovery.

Keywords: Space flight dynamics, reusable launch vehicles, trajectory, orbit.

1. Introduction

The main difficulty in achieving full reusability for launch systems comes with recovering the stages dropped by multiple stage launch systems. While, for example, the boosters of the Space Shuttle were reusable their recovery involved a difficult and sometimes futile search for them in the Atlantic Ocean. Similarly, the external tank burned up on re-entry.

One way to achieve full reusability of Launch Systems would be for every stage to be designed in such a way that after it has been jettisoned it can achieve a controlled glide that would allow for it to be flown in a region where its recovery would be much simplified.

A further simplification would be if the component of the RLS (Reusable Launch System) would be recovered while in flight instead of being allowed to land in water or on the ground. In this way recovery can be achieved in a predetermined position and with a great reduction in cost as the recovery would not include a search operation.

To maximize the launched payload the RLS components should be designed in such a way that the minimum amount of mass is set aside for recovery. Thus, so

[1] Eng., Institutul National de Cercetari Aerospatiale “Elie Carafoli” INCAS (National Institute for Aerospace Sciences), PhD Candidate Aerospace, University POLITEHNICA of Bucharest, Romania

[2] Dr. Eng., Institutul National de Cercetari Aerospatiale “Elie Carafoli” INCAS (National Institute for Aerospace Sciences)

called Fly-Back methods as proposed by Space X Falcon which involves the vertical landing on a barge is less than optimal as a part of the fuel has to be saved for landing. Similarly recovering after the RLS component deployed a parachute is again less then optimal as the mass of the parachute takes away from fuel.

Thus, the optimum solution is to streamline the RLS components and equip them with aerodynamic control surfaces such that their trajectory can be controlled and stabilized at an altitude and speed where a specifically designed aircraft can rendezvous and couple with them and then guide them to a controlled conventional landing.

Such an approach is being studied at the DLR institute by the SART (Space Launcher Systems Analysis) group, under the name In-Air capturing, which aims to work in conjunction with the group's Liquid Fly-back Booster (LFBB) initiative [10], [11], [12]. The LFBB is a design for Liquid Fuel booster, to be used with Arianne 5, which has a winged design and is meant to Fly Back after being jettisoned. This was conceived to allow the LFBB to attach itself to a towing cable carried by a specially equipped Boeing 747, which would then tow the LFBB in the vicinity of the landing strip. This whole approach allows the LFBB to conserve a smaller amount of fuel for the trip back then if it was meant to reach the landing strip by itself. However, this method is not very versatile as it is sized for a heavy launcher like Arianne 5 and because of the use of a Boeing 747, with its large size and fuel consumption becomes less and less economically feasible the smaller the launcher taken into consideration. The concept also requires extensive automation to be installed on the RLS component as the recovering aircraft is meant to have a completely passive role in the recovery process [12] which increases the costs because of the needed avionics, software and supplemental sensors, that would be needed to allow the RLS component to autonomously detect, identify, track and intercept the recovering platform, which seems counter-productive even with a Reusable booster as it would still be an expandable component.

We aim for a different approach to the same basic concept of recovering RLS components while still airborne. The proposed method is usable on a larger number of RLS sizes and would also shift the cost of the extra avionics and equipment to the airborne recovering platform which is more economically feasible. Thus, the approach we propose rests on two concepts:

First: all components of the RLS use wings and/or are streamlined, equipped with aerodynamic control surfaces and controllable. Thus not only the boosters but also the intermediate stages and orbiter/re-entry vehicle would have a capacity to perform a control glide in the atmosphere. Naturally this capacity would be confined to high-speeds due to the need for the RLS components to be optimized for supersonic and hypersonic speeds because of their main missions. This would introduce the need for the second concept.

Second: to use a specially designed UAV to perform the recovery of the RLS component. The Recovery UAV (from henceforth titled RUAV) would approach the RLS component, gliding at high altitude and high subsonic speeds, and would attach itself to the RLS component.

The current paper presents initial results relating to the first concept. Namely studies regarding the feasibility of implementing a post-jettisoning trajectory for an RLS component such that it achieves a predetermined stable flight condition.

2. Used method

The motion equations were implemented in the software package ASTOS which is approved by European Space Agency (ESA) for space craft trajectory computations. In order to set up the numerical simulations there are several settings to consider.

The central celestial body, the Earth, is modeled as a flattened spheroid and is defined as presented in table 1:

Table 1

Central Body Parameters

Parameter	Value
Equatorial radius	6378.135 km
Polar radius	6356.912 km
Gravity parameter	398602 km^3/s^2
Non-dimensional zonal harmonic, J2	0.0010827

The gravitational potential of an oblate spheroid is approximated as a function of radius R and declination δ, and expanded into spherical harmonics of 2nd order, [9].

The local acceleration of gravity is the gradient vector of the potential function along the local axis system, [9]:

$$\hat{G} = \nabla U = \begin{bmatrix} \dfrac{\partial U}{\partial R} \\ \dfrac{1}{R\cos\delta}\left(\dfrac{\partial U}{\partial \lambda}\right) \\ \dfrac{1}{R}\left(\dfrac{\partial U}{\partial \delta}\right) \end{bmatrix}_L \tag{2}$$

The spin state of the Earth is defined by the direction of North and the location of the prime meridian following the definition of the IAU (International Astronomical Union).

The geometrical and aerodynamic model used for the numerical simulations is based on the Hermes vehicle with the following characteristics:

- Lifting surface – 73 m^2;
- Reference length – 10 m;
- Weight – 16 000 kg.

The aerodynamic model used to determine the aerodynamic forces takes a range of Mach numbers from 2.5 to 30 and angle of attacks respectively 10° and 40°, [8].

$$\hat{F} = qA_{ref}\begin{bmatrix} -C_D(M,\alpha) \\ 0 \\ -C_L(M,\alpha) \end{bmatrix}_A \tag{3}$$

The atmospheric model used is US 76, [4], [5], which assumes that the pressure, temperature, density and viscosity change with altitude.

The motion equations are functions of six state variables. Three state variables specific to the vehicle position, three auxiliary state variables that define its speed. The position of the vehicle is specified by a set of spherical coordinates fixed on the planet (R, λ, δ). As shown in *Fig. 1*, R represents the distance from the center of the plant, λ the eastern longitude measured from the Greenwich meridian and δ the declination measured from the equatorial plane.

The state variables (V, γ, χ) define the magnitude and direction of the flight path velocity vector relative to the local reference system, L: V is the flight path velocity, γ is the flight path inclination, and χ is the azimuth in the direction flight or angle of inclination, in relation to the North, [3]. The Cartesian vector components along the local system are given by:

$$\hat{V}_k = V\begin{bmatrix} \sin\gamma \\ \cos\gamma\sin\chi \\ \cos\gamma\cos\chi \end{bmatrix}_L \tag{4}$$

This representation of state variables is undetermined above the planet's poles and for vertical flight, where the definition of North is ambiguous. In both cases, the value of χ is indefinite.

The state kinematic equations represent the kinematic relations established by position definition and velocity state variables:

$$\frac{d}{dt}\begin{bmatrix} R \\ \lambda \\ \delta \end{bmatrix} = \begin{bmatrix} V\sin\gamma \\ \dfrac{V\cos\gamma\sin\chi}{R\cos\delta} \\ \dfrac{V\cos\gamma\cos\chi}{R} \end{bmatrix} \tag{5}$$

Dynamic equations result from Newton's second law, [7]:

$$\frac{d}{dt}\begin{bmatrix} V \\ \gamma \\ \chi \end{bmatrix} = \begin{bmatrix} X + \Omega_E^2 R\cos\delta\left(\cos\delta\sin\gamma - \sin\delta\cos\gamma\cos\chi\right) \\ -\frac{1}{V}Z + \frac{V}{R}\cos\gamma + 2\Omega_E\cos\delta\sin\chi + \frac{\Omega_E^2 R\cos\delta}{V}\left(\cos\delta\cos\gamma + \sin\delta\sin\gamma\cos\chi\right) \\ \frac{Y}{V\cos\gamma} + \frac{V\cos\gamma}{R}\tan\delta\sin\chi + 2\Omega_E\left(\sin\delta - \cos\delta\tan\gamma\cos\chi\right) + \frac{\Omega_E^2 R\cos\delta\sin\delta\sin\chi}{V\cos\gamma} \end{bmatrix} \tag{6}$$

where Ω_E is the angular velocity of the planet with respect to the z axis of the planeto-centric reference system. X, Y, Z are the components of the acceleration along the axis of the reference system.

Acceleration that acts on the vehicle results from gravitational force, aerodynamic force and thrust force.

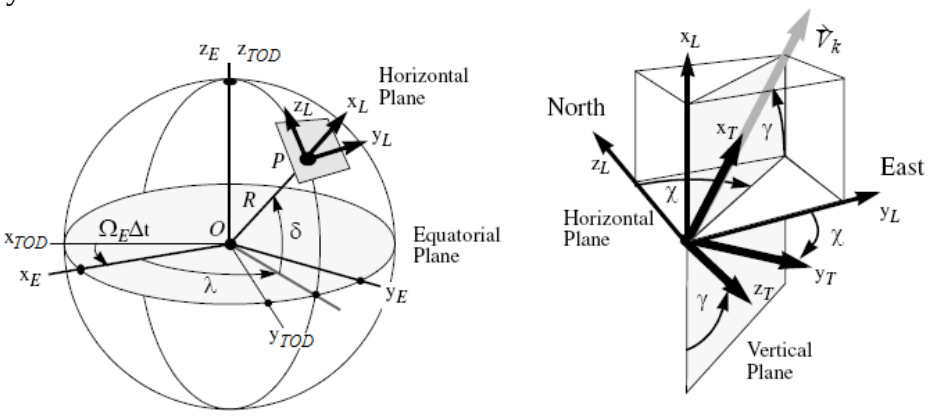

Fig. 1 Definition of the planet-relative position and flightpath state variables [3]

The attitude of the vehicle along the flight path can be defined by a set of aerodynamic angles:

- Incidence angle α;
- Lateral slip angle β;
- Lateral inclination angle μ_a.

The side slip angle is optional and its default value is set to zero ("reduced" aerodynamic angles).

The aerodynamic angles have the following dynamic equations [3]:

$$\dot{\alpha} = -P\cos\alpha\tan\beta + Q - R\sin\alpha\tan\beta + \frac{\cos\mu}{\cos\beta}\left[\dot{\delta}\cos\chi - \dot{\gamma} + (\dot{\lambda} + \Omega_E)\cos\delta\sin\chi\right]$$
$$+ \frac{\sin\mu}{\cos\beta}\left[\dot{\delta}\sin\chi\cos\gamma - \dot{\chi}\cos\gamma(\dot{\lambda} + \Omega_E)(\sin\delta\cos\gamma - \cos\delta\cos\chi\sin\gamma)\right] \tag{7}$$

$$\dot{\beta} = P\sin\alpha + R\cos\alpha + \sin\mu\left[\dot{\delta}\cos\chi - \dot{\gamma} + (\dot{\lambda} + \Omega_E)\cos\delta\sin\chi\right] \tag{8}$$
$$+ \cos\mu\left[\dot{\chi}\cos\gamma - \dot{\delta}\sin\chi\sin\gamma + (\dot{\lambda} + \Omega_E)(\cos\delta\cos\chi\sin\gamma - \sin\delta\cos\gamma)\right]$$

$$\dot{\mu} = P\cos\alpha\cos\beta + Q\sin\beta + R\sin\alpha\cos\beta - -\dot{\alpha}\sin\beta + \dot{\chi}\sin\gamma + \dot{\delta}\sin\chi\cos\gamma \tag{9}$$
$$-(\dot{\lambda} + \Omega_E)(\cos\delta\cos\chi\cos\gamma - \sin\delta\sin\gamma)$$

where P, Q, R are the position vector components, γ is the flight path inclination, δ is the declination, λ is the est longitude, χ is the flight path azimuth and Ω_E is the angular velocity of the Earth.

The thrust vector in the local axis coordinate system (L) is calculated as, [7], [8]:

$$\hat{F}_{thrust} = T_A^L T_B^A \sum_{i=1}^{n} \hat{T}_i \tag{10}$$

where $\hat{T}_i$ is the thrust of each propulsion system given in the vehicle coordinate system (B) and "i" represents the number of engines. Moreover, the aerodynamic force is given by:

$$\hat{F}_{Aero} = T_A^L T_B^A \hat{F} \tag{11}$$

depending on the coordinate system in which $\hat{F}$ is given.

Transformation from the reference system fixed to the vehicle, (B), to the trajectory coordinate system (A), is defined by:

$$T_B^A = T_3(\beta)T_2(-\alpha) \tag{12}$$

where α and β denote the angle of incidence and respectively, the lateral inclination angle. For the transformation from the reference system (A) to the local coordinate system (L), the following equation is used:

$$T_A^L = T_1(\chi_a)T_2\left(\frac{\pi}{2} - \gamma_a\right)T_1(-\mu_a) \tag{13}$$

where γ_a and χ_a are the inclination of the trajectory and the orientation angles, and μ_a is the lateral inclination angle of the trajectory. The inclination and

the position of the trajectory are defined by the velocity vector a, while the lateral inclination angle is controlled.

3. Case studies

For the studies performed, a series of three numerical simulations of the reentry trajectories were provided with the objective of validating reentry strategies of a reusable vehicle:

-Re-entering the Earth's atmosphere by controlling only the incidence angle;

-Re-entering the earth's atmosphere by controlling both the incidence angle and the lateral inclination angle;

- Suborbital re-entry from 60 km altitude using a VEGA rocket launch.

The reusable vehicle used in this phase of the study was Hermes due to the similarity to the vehicle concept proposed in the project. The numerical simulations are defined based on the following: the determination of the central body model, the atmospheric model, the aerodynamic model and the vehicle. The dynamic model considers the initial state of the numerical simulation, as follows:

For the first two cases the initial state includes the orbital elements of the orbit where the re-entry maneuver is initiated and an initial deorbitation which is defined as the trajectory arc taken upon leaving orbit.

Table 2

Orbital states at the start of deorbitation maneuver

Initial states	Value
Semi-major axis	6878.135 km
Eccentricity	0
Inclination	51.5 degrees
Periapsis argument	0 degrees
Right ascension of the ascending node (RAAN)	34.0 degrees
True anomaly	0 degrees

Table 3

Re-entry arc states

Initial Deorbitation	Value
Periapsis altitude	65 km
Re-entry altitude	120 km
Target longitude	-65 degrees
Target latitude	5 degrees
Estimated downrange	5000 km
Estimated downrange time	1000 seconds

In the third case a suborbital flight is considered based on the VEGA launch trajectory toward a circular polar orbit at 700 km altitude and 90 degrees inclination. The last two rocket stages, Zefiro 9 and AVUM plus the payload, were replaced with the Hermes vehicle taking into account the similar masses in order to numerically simulate a suborbital launching trajectory of the vehicle at an altitude of 60 km. This was done to approximate the trajectory taken by a recoverable

intermediary stage. The initial state for this case includes only the orbital elements as follows:

Table 4

Sub-orbital flight parameters

Parameters	Value
Semi-major axis	3779.77 km
Eccentricity	0.75
Inclination	83.44 degrees
Periapsis argument	-166.52 degrees
Right ascension of the ascending node (RAAN)	47.05 degrees
True anomaly	173.8 degrees

For the aerodynamic model, a 3-degrees of freedom model was chosen for all three cases. This implies that besides the translational motion equations only the angle of incidence and the angle of lateral inclination are considered as control parameters. At the same time, the method of estimating the heat flow is defined as supersonic convective flux given by parameters:

- Heat flow constant - 0.000164;
- Density exponent - 0.5;
- Expression of speed - 3.0.

Incidence angle variation is an input parameter and is defined as a Mach function with a linear interpolation function:

Table 5

Mach number versus AoA

Mach	Angle of Attack (degrees)
2.0	23.0
2.5	23.0
8.0	31.0
10.0	34.0
12.0	35.0
40.0	35.0

The angle of lateral inclination is defined as a linear control law between 70 and 80 degrees. Since the reentry vehicle is not equipped with supplementary fuel for the re-entry phase, a single flight phase is set in which the vehicle glides and the parameters (angle of attack and/or sideslip angle) are changed in order to achieve the target parameters: altitude 10 km and Mach number of 0.85.

Besides the target altitude and Mach number, other parameters have been taken into account as constraints:

- Maximum heat flux density: 440kW/m^2;
- Maximum dynamic pressure: 14400 Pa.

4. Results

The first case is based on an orbital re-entry of the spacecraft in the Earth's atmosphere with a single control parameter which is the angle of attack as seen in Fig. *6*.

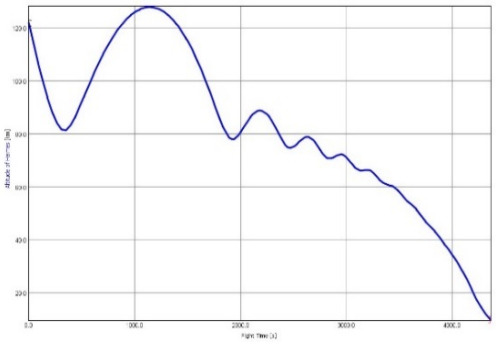

Fig. 2 Altitude vs flight time

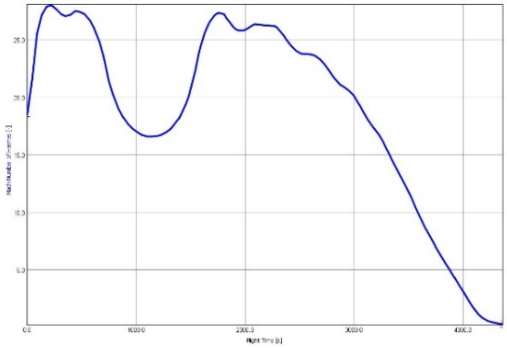

Fig. 3 Mach number vs flight time

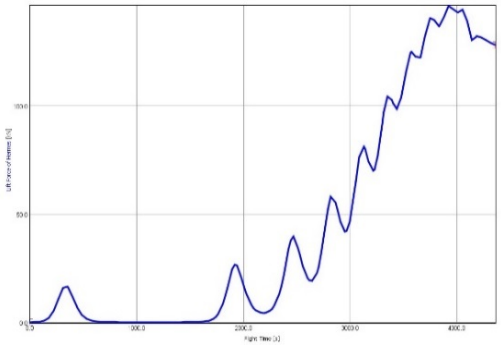

Fig. 4 Lift vs flight time

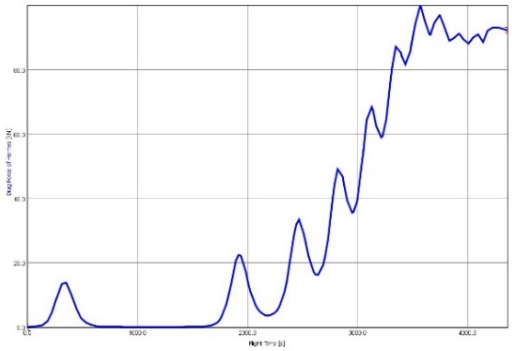

Fig. 5 Drag vs flight time

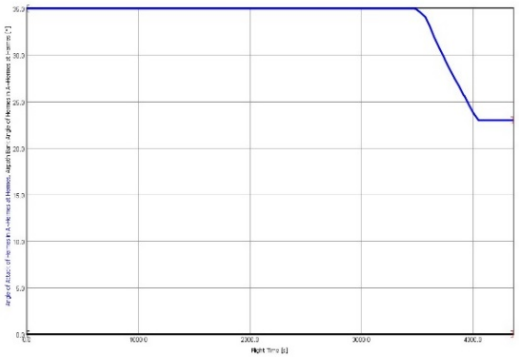

Fig. 6 AoA and Bank angle vs flight time

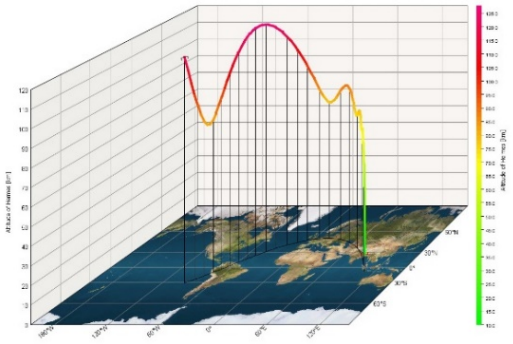

Fig. 7 3D view

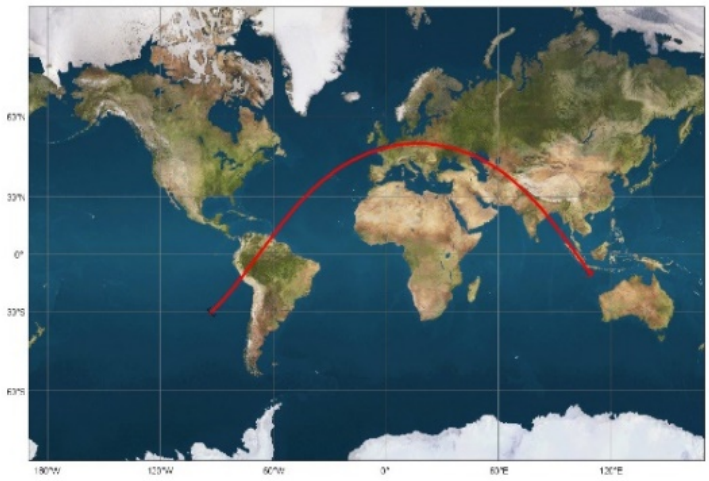

Fig. 8 Groundtrack view

Fig. 9 Satellite view

The second case studied is based on the same structure as the first with the difference that the second control parameter, the bank angle, is activated, so that the reentry is a direct one, and the vehicle is not rejected by the atmosphere as seen in Fig. 10 compared to Fig. 2.

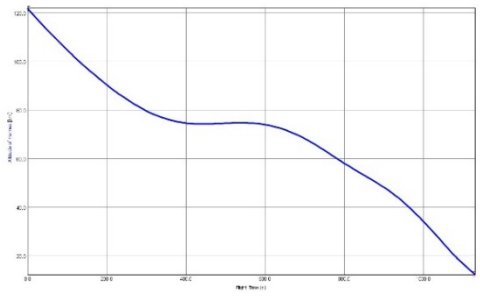

Fig. 10 Altitude vs flight time

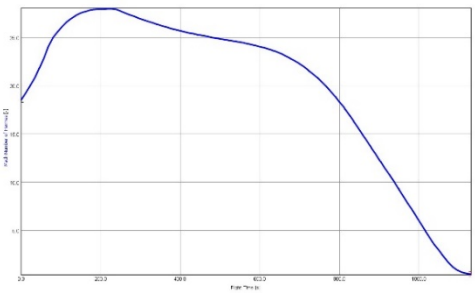

Fig. 11 Mach Number vs flight time

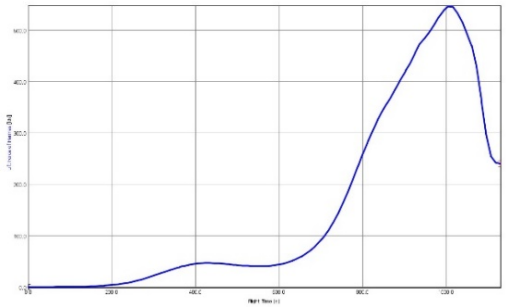

Fig. 12 Lift vs flight time

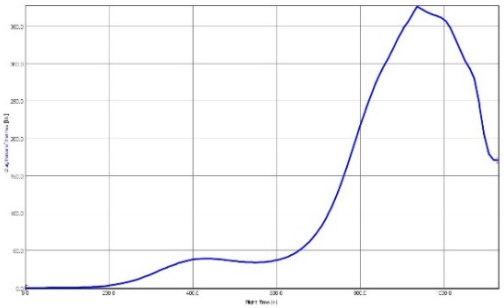

Fig. 13 Drag vs flight time

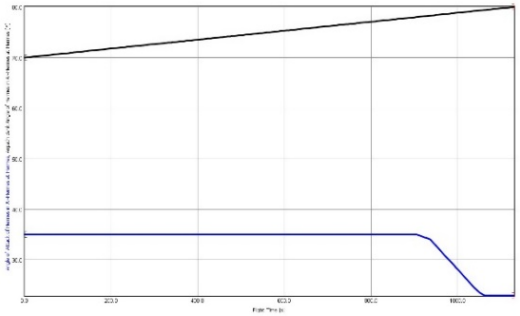

Fig. 14 AoA and Bank angle vs flight time

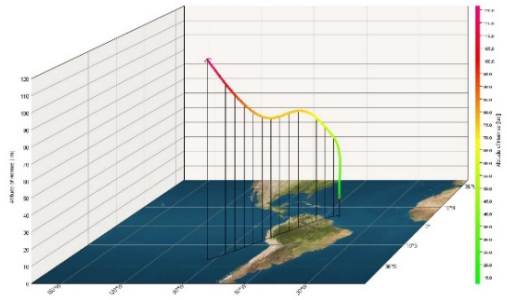

Fig. 15 3D view

Fig. 16 Groundtrack view

Fig. 17 Satellite view

The last case is based on the VEGA missile launch trajectory toward a circular polar orbit and the scenario starts at 60 km altitude with the jettisoning of Hermes as seen in Fig. 18.

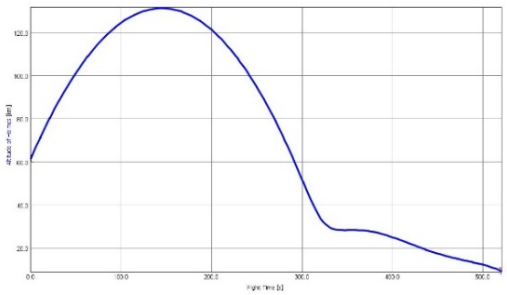

Fig. 18 Altitude vs flight time

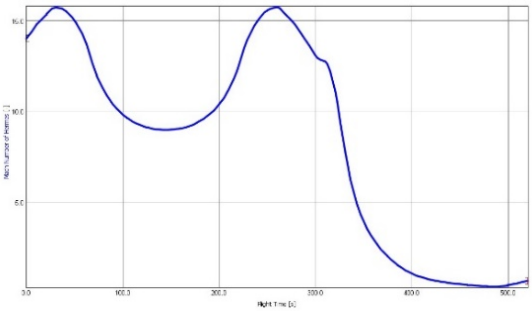

Fig. 19 Mach Number vs flight time

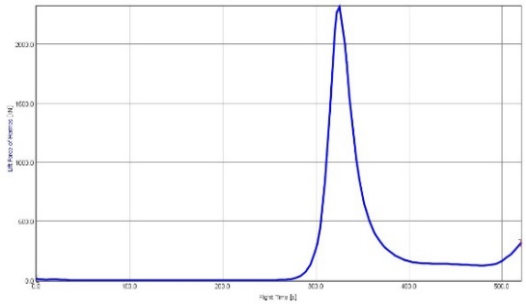

Fig. 20 Lift vs flight time

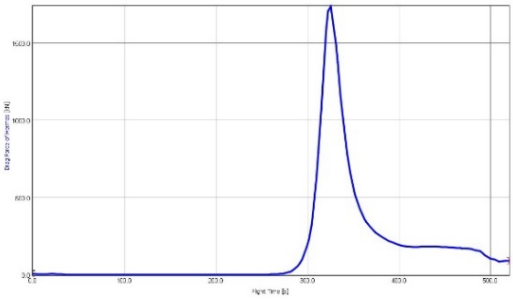

Fig. 21 Drag vs flight time

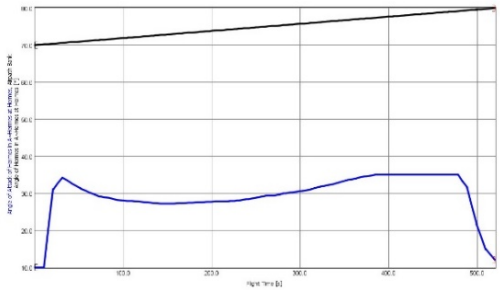

Fig. 22 AoA and Bank angle vs flight time

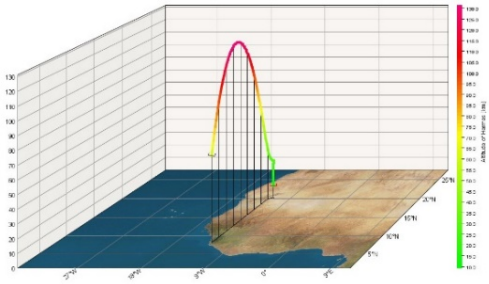

Fig. 23 3D view

Fig. 24 Ground track view

Fig. 25 Satellite view

5. Conclusions

The present work analyses re-entry strategies of reusable space vehicles using the Hermes shuttle as a stand in. This choice came about due to the similarities between Hermes and the concept studied in the project proposed by the authors.

Target parameters for reentry analysis were to reach an altitude of 10 km and a Mach number of 0.85.

From the results of the first preliminary re-entry analysis in which only the incidence angle was used as a control method it can be seen, that the shuttle did not have a direct reentry. The reentry speed coupled with the incidence angle is not enough to brake and the shuttle is rejected by the atmosphere, the reentry phase duration being much longer and thus the precision of the reentry maneuver decreases drastically.

The second analyzed case uses, together with the incidence angle, the lateral inclination angle as a control parameter of the trajectory. The results show that the duration of the re-entry maneuver is only 1165 seconds being a direct reentry.

The last case under consideration is actually a suborbital flight starting at 60 km altitude due to the jettisoning of the reusable vehicle after the full burn of the first two stages of the VEGA launcher. Due to the initial impulse given by the VEGA launcher, the vehicle describes a circle arc up to 130 km altitude, then starts the descent phase to the 10 km target altitude. In this case the initial Mach number is much smaller than in the two cases of orbit reentry, 15.7 Mach vs. 28 mach. The results show two peaks at the Mach 15.7 due to the ascending trajectory given by VEGA.

Thus, by analyzing the re-entry methods, the next phase of the work will include analyses in detail of the trajectories necessary for the reusable vehicle to be intercepted by the UAV platform at the 10 km altitude with a speed of 0.85.

R E F E R E N C E S

[1] *C. Weiland*, "Computational Space Flight Mechanics", Berlin, 2010
[2] Vega User's Manual, Issue 4, Revision 0, April 2014
[3] ASTOS User Manual.
[4] U.S. Standard Atmosphere, 1976, NOAA, NASA, US Air Force, Washington, D.C., 1976;
[5] *ANSI/AIAA G-003B-2004, Guide to Reference and Standard Atmosphere Models, 2004*
[6] *Seidelmann P. K., Abalakin V. K., Bursa M., Davies M. E., de Bergh C., Lieske J. H., Oberst J., Simon J. L., Standish E. M., Stooke P. and Thomas P. C.*, Report of the IAU/IAG Working Group on Cartographic Coordinates and Rotational Elements of the Planets and Satellites: 2000, Celestial Mechanics and Dynamical Astronomy, **Vol. 82**, No. 1, January 2002

[7] *Roenneke, A. J.*, Atmospheric Flight Dynamics Based on Flight-Path Coordinates, Institute of Flight Mechanics and Control, University of Stuttgart, Rept. IFR TR 95-08, July 1995

[8] *Roenneke, A. J.*, ALTOS-2 Reentry Problem Set, Advanced Launch and Reentry Trajectory Optimization Software Documentation, Technical Report, Institute of Flight Mechanics and Control, University of Stuttgart, Rept. IFR TR 95-06, Jan. 1995

[9] *Escobal P. R.*, Methods of Orbit Determination, Krieger Publ., Malabar, Fl., 1976

[10] *S.V. Antonenko and S. A. Belavskiy*, "Mid-Air Retrieval technology for returning of reusable launch vehicles' boosters," in Progress in Propulsion Physics, EDP Sciences, 2009, pp. **Vol. 1**, pp. 481-494.

[11] *M. Sippel*, "Concurrent Launcher Engineering at DLR," in Concurrent Engineering Workshop, ESTEC, Noordwijk, Holland, 2004.

[12] *M. Sippel, J. Klevanski*, "Progresses in Simulating the Advanced In-Air-Capturing Method.," in 5th International Conference on Launcher Technology, Missions, Control and Avionics, 2003